The activation of black holes and their accretion rates are linked to both star formation and bulge types.

Hassen M. Yesuf

Sandra Faber, David C. Koo, Joanna Woo, Yifei Luo, Joel Primack

Kavli Institute of Astronomy & Astrophysics, Peking University
Kavli PKU/IPMU Fellow

January 10, 2019

What quenches star formation?

- The mechanisms for build-up of bulges include galaxy mergers (Toomre & Toomre 72; Hopkins+09), slow secular evolutions such as bars (Kormendy & Kennicutt 04), and violent clumpy disk instabilities (Noguchi 1999; Elmegreen+08; Dekel+09).

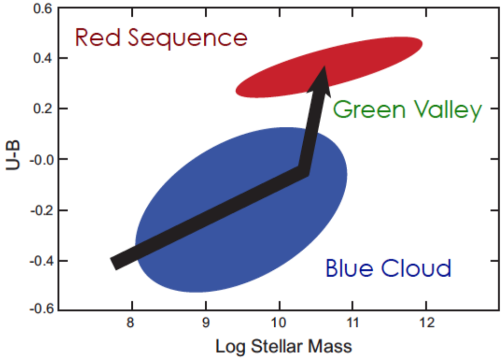

What is a bulge ?

- "A rounded swelling which distorts an otherwise flat surface." The Oxford dictionary
- A bulge has different isophotes (e.g., position angle and ellipticity) compared to the surrounding disk.
- Excess light above the inward extrapolation of the exponential light profile of a disk component.

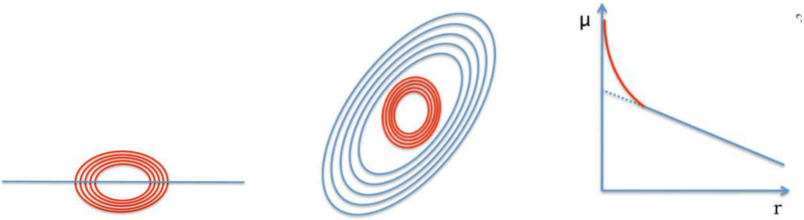

Figure: Bulge definitions (Gadotti 2012).

Two types of bulges: classical and pseudobulges

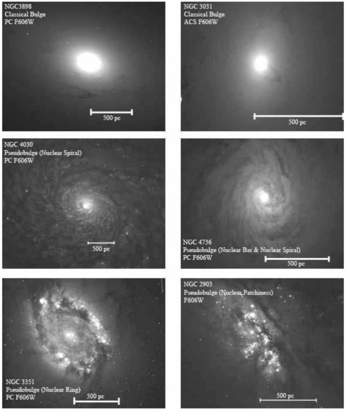

Figure: Classical bulges have smooth featureless isophotes while pseudobulges show nuclear bars, nuclear rings, spiral structure, or patchy star formation within ~ 1 kpc (Fisher & Drory 2010).

There are two types of bulges: more example

- The common view is that classical bulges are formed mainly by dissipative mergers of galaxies, while pseudobulges are formed by disk related secular processes internal to galaxies.
- Sersic profile $I(r) = I_e \exp\left\{b_n\left[(r/r_e)^{1/n} - 1\right]\right\}$

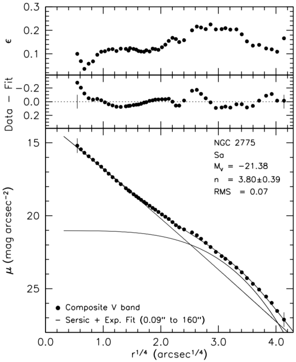

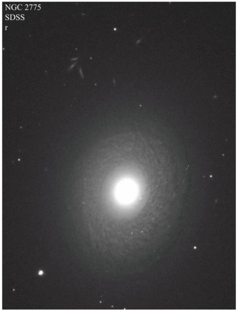

There are two types of bulges: more example

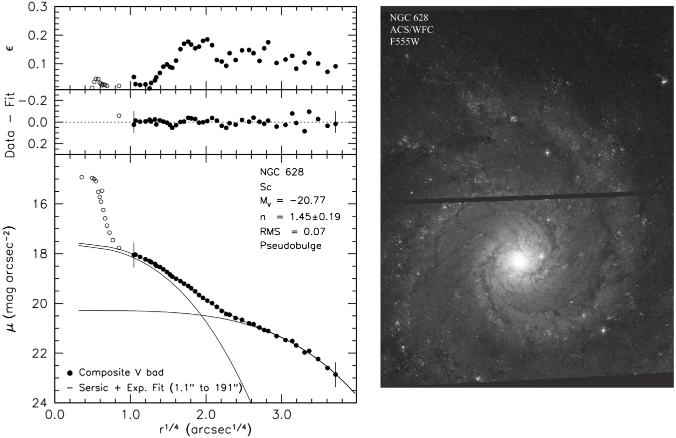

Figure: Example pseudobulge

Why do we care about bulge types ? Better understanding of galaxy formation.

- The high frequency of pseudobulges in massive galaxies in local universe **hints a problem with our theory of galaxy formation by hierarchical clustering**. Within 8 Mpc of our Galaxy. Kormendy+10 found that at least 11 out of 19 galaxies show no evidence for classical bulges. Galaxy mergers are are frequent enough that these massive galaxies should have classical bulges (Peebles & Nusser 2010; Kormendy et al. 2010).

Why do we care about bulge types ? Better understanding black hole feeding & feedback.

- Unlike ellipticals and classical bulges, pseudobulges do not obey the tight correlations between black hole mass and the host bulge properties (e.g., velocity dispersion). This suggests **different black hole feeding processes for the different bulge types** (Kormendy & Ho 2013).

Simulations find AGN feedback plays a role in size and structure evolution of massive galaxies.

- AGN feedback arising from BAL winds and X-ray radiation, can reduce the central density within 1 kpc, and enhance the size growth of massive galaxies (Choi+18).

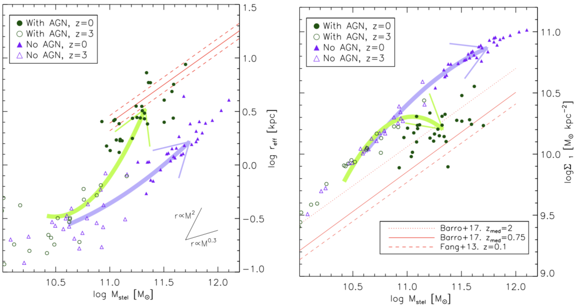

Figure: Left: Mass vs. size. right: Mass vs. $\Sigma_1 = M(r < 1kpc)/\pi(1kpc)^2$

Summary of what I did

- I use machine learning to classify galaxies into real bulges and pseudobulges using the bulge-types of 809 representative galaxies from the SDSS by Gadotti (2009).
- Use structural and stellar population predictors that can easily be measured without image decomposition.
- Classify about 45,000 face-on SDSS galaxies above 10^{10} $M_{\odot}$ into real bulges or pseudobulges with high accuracy.
- Study the effect of bulge type on AGN activation (fraction) and accretion onto black holes.

Gadotti 2009's criteria of classifying bulges.

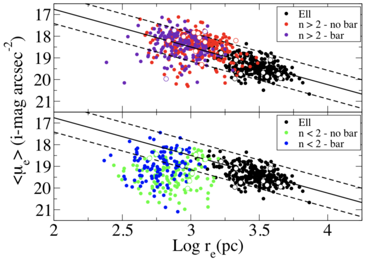

- The two common structural criteria for bulge classification are Sérsic index of the bulge ($n_{\rm bulge}$, Fisher & Drory 2008) and deviation from the Kormendy relation (Gadotti 2009).
- The two definitions are related but different.
- There is no single ideal way of identifying bulge-types; a new approach is needed.

Introduction: Decision tree classifier

- Gini impurity (GI) measures of how often a randomly chosen element would be incorrectly labeled if it was labeled according to the distribution of labels in a subset.
- $GI = \sum_{i=1}^{J} p_i \sum_{k \neq i} p_k = 1 - \sum_{i=1}^{J} {p_i}^2$ (e.g., $J = 2$, red or blue).

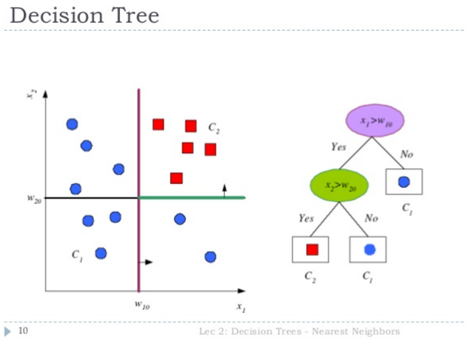

An example decision tree for a bulge classification

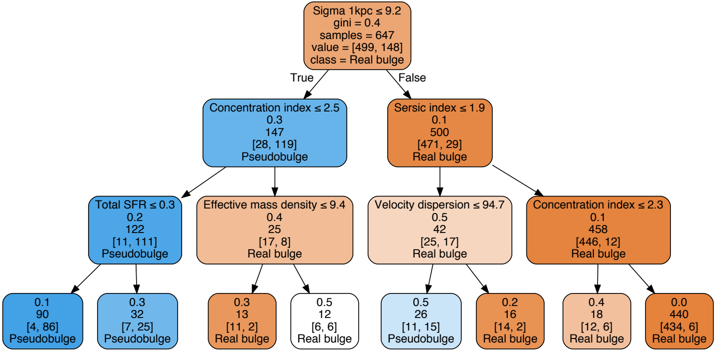

An example decision tree for a bulge classification

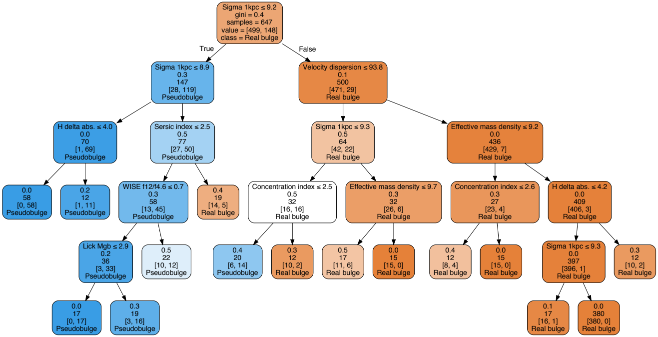

An example decision tree for a bulge classification

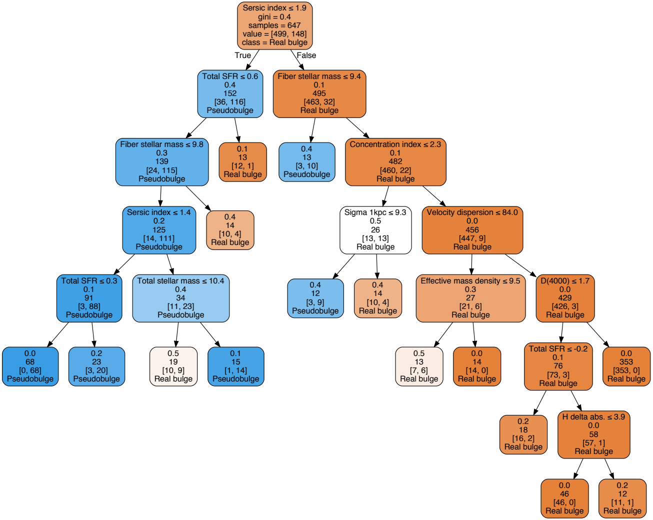

The Random Forest algorithm: grow less correlated and independent tree for better prediction

- Grow each tree on an independent bootstrap sample from the training data.
- At each node, randomly select m of the n variables and find the best split on the selected m variables.
- Combine information (average) from different trees to get better predictions.

Sample property: Classifying a large sample of SDSS galaxies.

.

Cut description	Criterion	Number of galaxies	Sample name
Redshift limit	$z = 0.02 - 0.07$	156,229	
Mass limit	$\log M_\star (M_\odot) = 10 - 12$	80,960	SDSS main sample
Face-on (ellipticity cut)	$e = 1 - b/a < 0.5$	49,390	
Not Broad line AGN	Balmer line width $\sigma < 300$ km s^{-1}	44,619	
Gadotti (2009)'s cuts	$z = 0.02 - 0.07$ $\log M_\star (M_\odot) = 10 - 12$ $e = 1 - b/a < 0.1$	809	Gadotti (2009)'s sample
	80% of Gadotti (2009)'s sample	647	Training sample
	20% of Gadotti (2009)'s sample	162	Test sample

The machine recovers bulge types with $93 \pm 2\%$ accuracy.

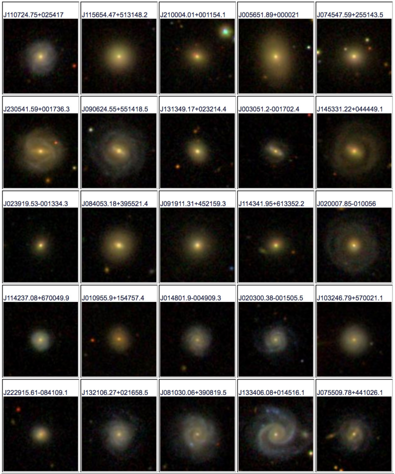

- Images of random galaxies from the training sample correctly classified by the Random Forest algorithm.
- The top three rows are real bulges and the bottom two rows are pseudobulges.

Will you agree with the machine?

- Which of these galaxies are pseudobulges or realbulges?

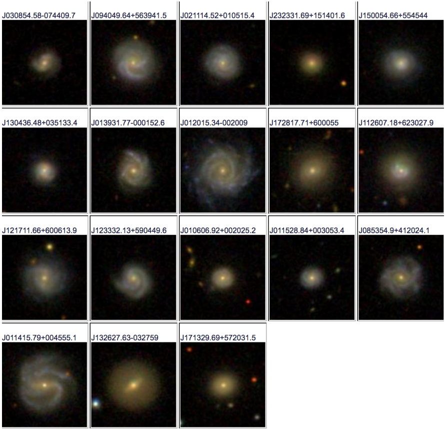

Will you agree with the machine?

- Which of these galaxies are real bulges or pseudobulges?

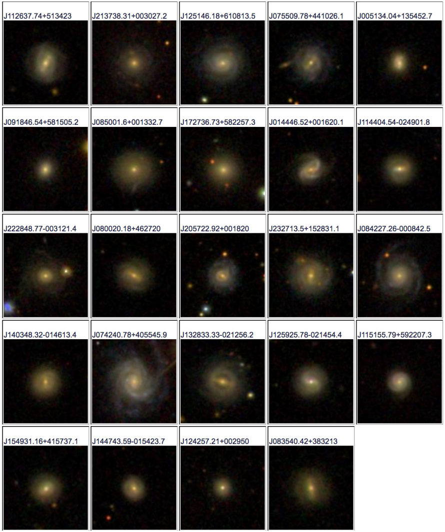

Which parameters are more important in recovering Gadotti's classification ?

- The RF algorithm hints that the central central mass density within 1 kpc, Σ_1, is at least as important as the concentration index and Sérsic index in predicting bulge-types.

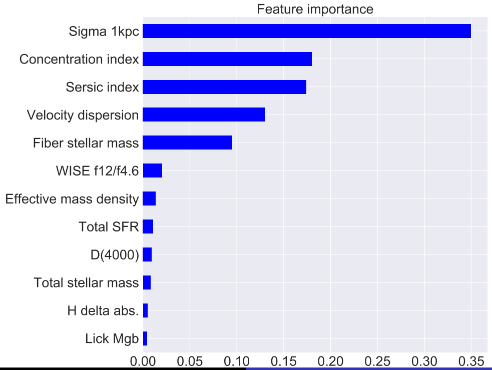

The RF classification maps well the bulge-types from the training to the predicted sample (1).

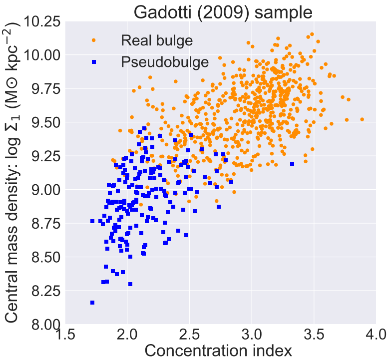

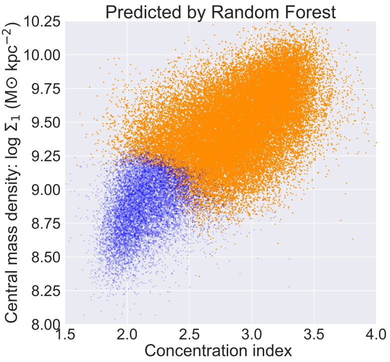

The RF classification maps well the bulge-types from the training to the predicted sample (2).

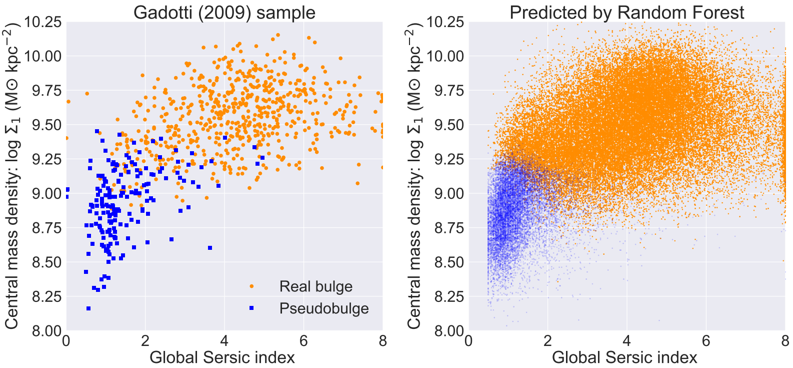

The RF classification maps well the bulge-types from the training to the predicted sample (3).

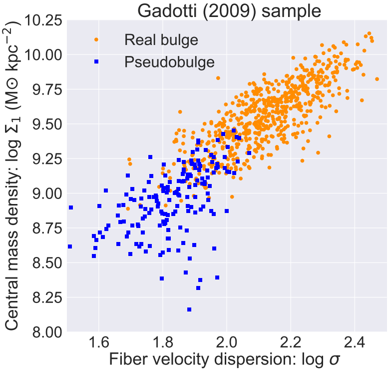

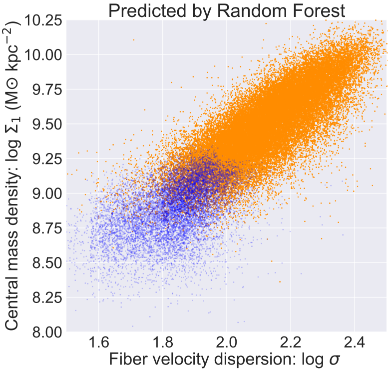

Black hole mass correlates with the bulge mass.

- The correlation arises as AGN-triggered outflows limit the gas reservoir for spheroid star formation (e.g., Silk & Rees 98)
- Black holes do not correlate with galaxy disks and with the properties of pseudobulges.
- Black holes are found in many bulgeless galaxies and bulges are not necessary for their formation.

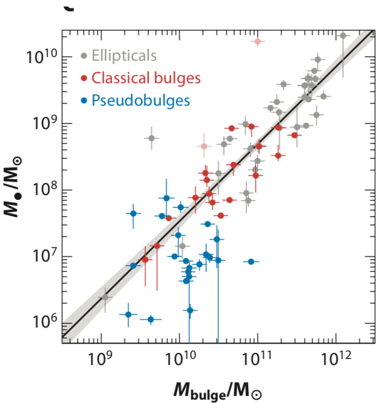

Figure: Kormendy & Ho 2013

Identifying AGNs with optical emission line ratios

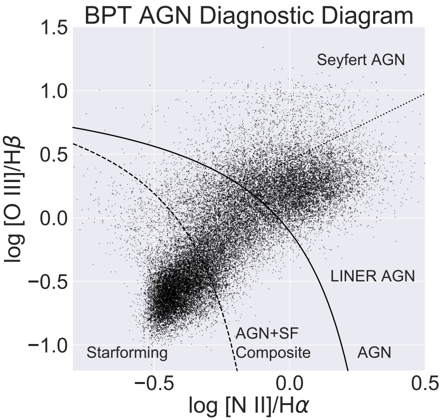

- AGNs emit high energy photons: O^{++} requires 35 ev while H^{+} 13.6 ev.
- More free electron produced by AGN also lead to stronger emission by collision with N^{+} and O^{++}.
- Require all 4 lines to have $S/N > 2$.
- 75% of AGNs are LINERs
- In each region, I compute the bulge fraction.

The fraction of galaxies with real bulges is higher when they host AGN

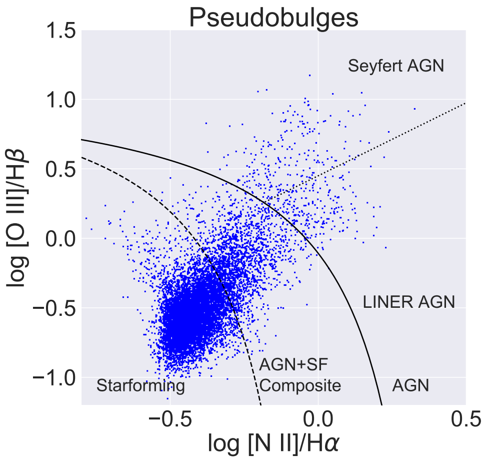

- $\sim$ 55% starforming galaxies are pseudobulges.
- $\sim$ 45% real bulges are starforming !

The fraction of galaxies with real bulges is higher when they host AGN

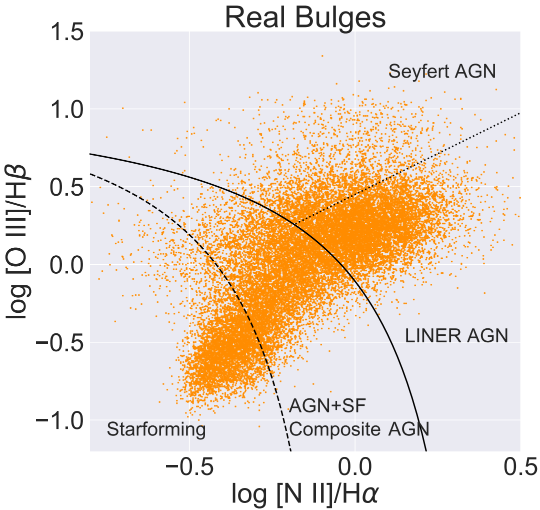

- $\sim 95\%$ of AGNs have real bulge hosts.
- $\sim 90\%$ of composite have real bulge hosts.

The pseudobulge fraction is lower for AGN host galaxies

Mass	AGN	AGN+SF Composite	Starforming (SF)	All
log $M < 10.5$	0.110 (0.087, 0.139)	0.271 (0.240, 0.305)	0.625 (0.582, 0.666)	0.341 (0.308, 0.375)
log $M > 10.5$	0.030 (0.015, 0.058)	0.074 (0.054, 0.101)	0.206 (0.176, 0.239)	0.057 (0.039, 0.083)
All	0.052 (0.035, 0.079)	0.092 (0.070, 0.120)	0.540 (0.500, 0.580)	0.211 (0.184, 0.241)

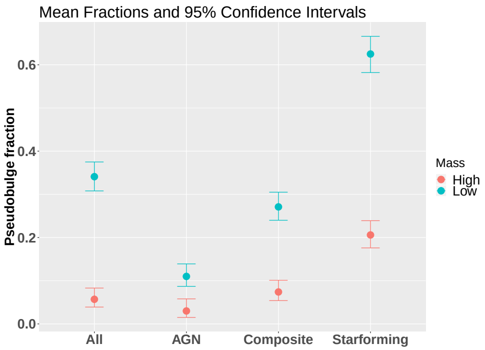

The pseudobulge fraction with Hα cut.

Photoionization by old stellar populations may explain H$\alpha < 3$Å without invoking AGN (Cid Fernandes +11).

Mass	All AGN (H$\alpha > 3$Å)	Seyfert (H$\alpha > 3$Å)	LINER (H$\alpha > 3$Å)	SF (H$\alpha > 3$Å)
log $M < 10.5$	0.220 (0.185, 0.259)	0.228 (0.190, 0.270)	0.202 (0.161, 0.250)	0.634 (0.590, 0.675)
log $M > 10.5$	0.062 (0.042, 0.091)	0.082 (0.058, 0.114)	0.073 (0.050, 0.105)	0.209 (0.179 0.242)
All	0.121 (0.096, 0.151)	0.146 (0.118, 0.180)	0.101 (0.076, 0.134)	0.549 (0.508, 0.589)

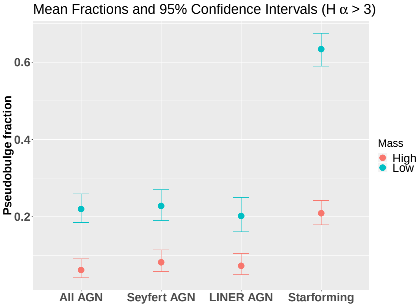

Dust correction

To use [O III] 5007 luminosity as an AGN accretion indicator, we dust correct it using the Hα/Hβ ratio and the emission-line extinction curve.

$$Q_\lambda = 0.6\,(\lambda/5500)^{-1.3} + 0.4\,(\lambda/5500)^{-0.7} \tag{1}$$

The optical depth at 5007Å relative to the V band is :

$$\tau_{5007} = \tau_V\, Q_{5007} \tag{2}$$

$$\tau_V = 0.921 \times \frac{2.5}{(Q_{4861} - Q_{6563})} \times \log \frac{H\alpha/H\beta}{3.1} \tag{3}$$

The dust corrected (dc) O3 luminosity is:

$$\text{Ł}_{\mathrm{O3,dc}} = L_{\mathrm{O3}} \times 10^{0.4\times 1.086\tau_{5007}} \tag{4}$$

Different AGN strength of the bulge types

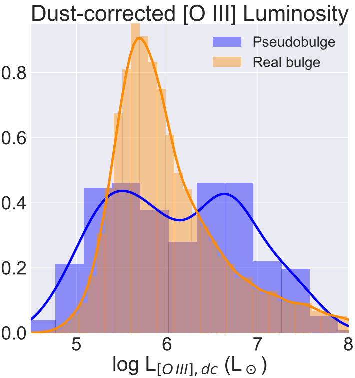

- The KS test indicates that the [O III] distributions are the same can be rejected at $> 5\sigma$ ($D = 0.2$ and p value ~ 0).
- The 16, 50, and 84 percentiles of $\log \ L_{\rm O3,dc}$ of pseudobulge AGNs are 5.3, 6.1, and 6.9 respectively.
- The percentiles for AGNs with real bulges are 5.5, 5.8, and 6.6.

The black hole mass fundamental plane relation

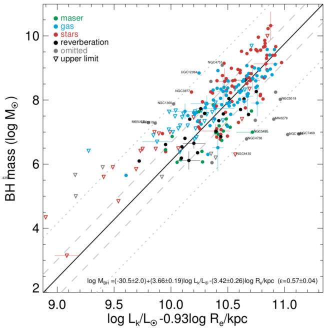

- The black hole masses can be estimated from stellar masses ($M_\star$) and half-mass radii ($R_{1/2}$) of the host galaxies (Van den Bosch 16),
- $\log M_{\rm BH}[M_\odot] = 7.48 + 2.91 \log\left(\frac{M_\star}{10^{11}\rm M_\odot}\right) - 2.77 \log\left(\frac{R_{1/2}}{5\rm kpc}\right)$.

Bulges on the mass-size relation

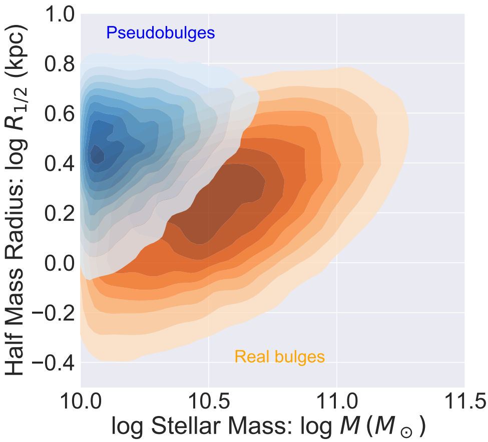

- Above the transition mass of $\sim 10^{10.5}$ $M_\odot$ real bulges dominated.
- Below $\lesssim 10^{10.5}$ $M_\odot$ real bulges are smaller than pseduobulges.

Pseudobulges have higher black hole mass

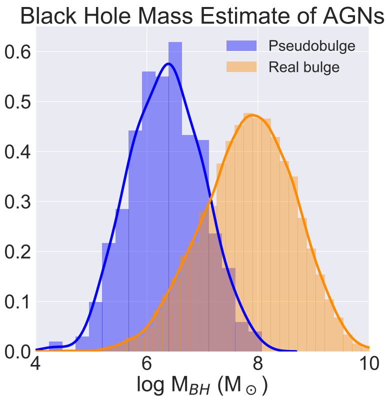

- The 16, 50, 84 percentiles of log $M_{\rm BH}$ for AGNs in pseudobulge hosts are 5.7, 6.3 and 7.0 respectively.
- For AGNs in real bulges are 7.0, 7.9, and 8.7 respectively.
- KS test indicates that the black hole mass distributions are significantly different ($D = 0.7$, p value ~ 0).

Pseudobulges have higher specific accretion rates

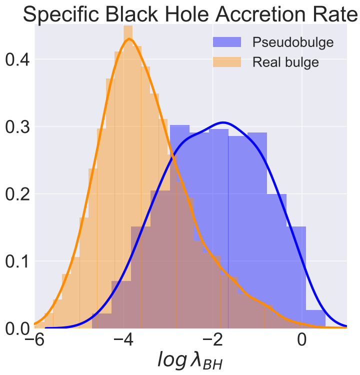

Figure: The normalized distributions of Eddington ratios.

- $\log \lambda_{\rm BH}$ is the bolometric luminosity divided by the Eddington luminosity, $L_{\rm Edd}$.
- Estimate the bolometric luminosity from the [O III] luminosity with a bolometric correction of $BC = 600$ (Kauffmann & Heckman 09).
- The 16, 50, 84 percentiles of $\log \lambda_{\rm BH}$ for the pseudobulges are -3.2, -1.9 and -0.76 while they are -4.8, -3.8, and -2.6 for real bulges.
- The $\log \lambda_{\rm BH}$ distributions are significantly different ($> 5\sigma$).

WISE mid-IR ratio correlates tightly with gas fraction for galaxies in COLD GASS survey.

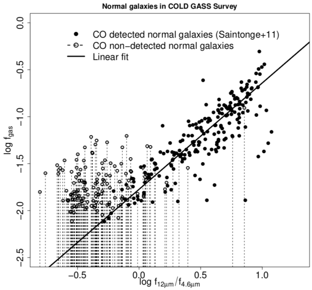

- The $f_{12}/f_{4.6}$ ratio is good SSFR indicator for AGNs and starforming galaxies (Donoso+12)
- Star-forming galaxies have high $f_{12}/f_{4.6}$ and quiescent galaxies have low $f_{12}/f_{4.6}$.
- The $f_{12}/f_{4.6}$ is an excellent proxy for the molecular gas fraction (Yesuf+17).
- The black line is the fit to the data and it includes the upper limits.

Availability gas may explain the accretion trend

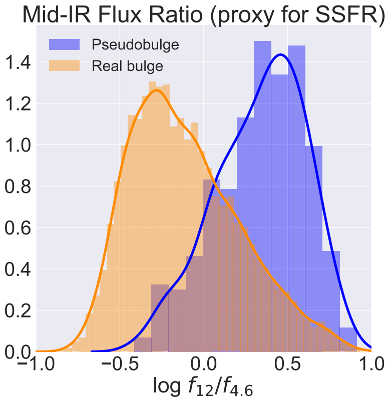

- The 16, 50, and 84 percentiles of $\log f_{12}/f_{4.6}$ for real bulges are -0.44, -0.16 and 0.23 and are 0.06, 0.38, and 0.61 for pseudobulges.
- These numbers may be converted to mean molecular gas fraction.
- $\log f_{12}/f_{4.6} = -0.2$ corresponds to $f_{\mathrm{H}_2} \sim 0.01$.
- $\log f_{12}/f_{4.6} = 0.5$ corresponds to $f_{\mathrm{H}_2} \sim 0.06$.

Bulge type/morphology may be important in determining AGN accretion rate.

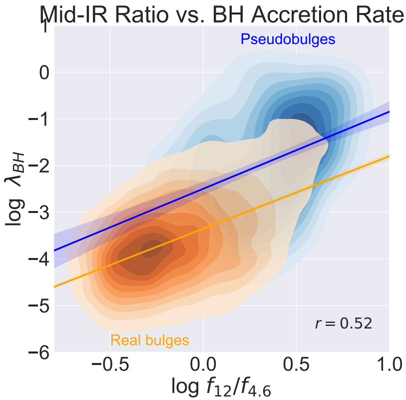

- AGN accretion is linked to both star formation and morphology.
- AGNs hosted by real bulges have a wide range of SSFR and $\lambda_{\rm BH}$. Most of them have low SSFR and low specific accretion rates.
- AGNs hosted by pseudobulges have higher star formation rates and higher $\lambda_{\rm BH}$.

Bulge type/morphology is may be important in determining AGN accretion rate.

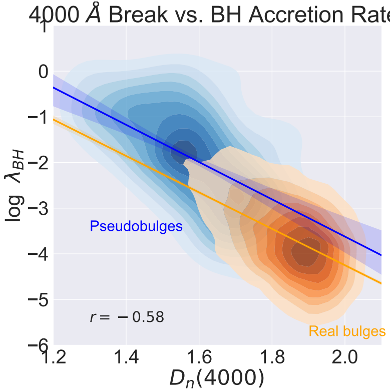

- AGN accretion is linked to both star formation and morphology.
- AGNs hosted by real bulges have a wide range of age/SSFR and $\lambda_{\rm BH}$. Most of them are old and have low accretion rates.
- AGNs hosted by pseudobulges are younger and have higher $\lambda_{\rm BH}$.

Bulge type is an important factor in determining AGN fraction (activation).

- AGN fraction at a given stellar mass and SSFR is generally higher by $\sim 2-3$ in real bulges than in pseudobulges.
- Low SSFR $< -11.5 \mathrm{yr}^{-1}$
- Medium SSFR -10.5 to $-11.5 \mathrm{yr}^{-1}$
- High SSFR $> -10.5 \mathrm{yr}^{-1}$

Mass	Type	Low SSFR	Medium SSFR	High SSFR
All mass	Pseudobulge	0.188 (0.149, 0.227)	0.099 (0.085, 0.113)	0.020 (0.017, 0.023)
	Real bulge	0.331 (0.325, 0.337)	0.273 (0.263, 0.283)	0.070 (0.064, 0.077)
$\log M < 10.0$	Pseudobulge	0.165 (0.125, 0.205)	0.086 (0.072, 0.100)	0.019 (0.016, 0.022)
	Real bulge	0.207 (0.199, 0.216)	0.217 (0.205, 0.230)	0.051 (0.044, 0.058)
$\log M > 10.5$	Pseudobulge	0.321 (0.199, 0.444)	0.174 (0.128, 0.220)	0.037 (0.023, 0.051)
	Real bulge	0.402 (0.395, 0.410)	0.340 (0.325, 0.356)	0.096 (0.085, 0.107)

Σ_1 may be used as a proxy for a black hole mass

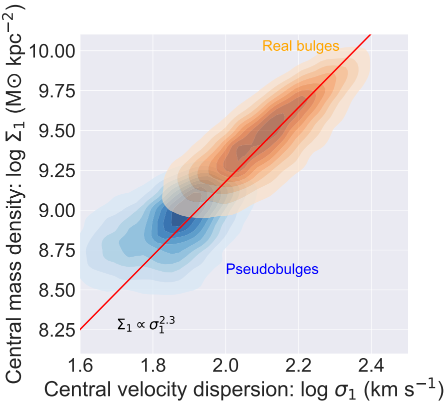

Regression Method	Real bulge only
Orthogonal Regression	$\alpha = 4.54 \pm 0.02$ $\beta = 2.31 \pm 0.01$
OLS Bisector	$\alpha = 5.61$ $\beta = 1.81 \pm 0.01$
Reduced Major Axis	$\alpha = 5.55$ $\beta = 1.83 \pm 0.01$
Weighted Least Square	$\alpha = 6.34 \pm 0.01$ $\beta = 1.47 \pm 0.01$

- If this relation is true at all times, Σ_1 is an easily measurable surrogate for the black hole mass.
- Using only real bulges from our new classification, we find that $\Sigma_1 \propto \sigma_1^{2.31\pm0.01}$, and using $M_{\rm BH} \propto \sigma^\alpha$, $\alpha = 4.38$ of Kormendy & Ho 2013 gives $M_{\rm BH} \propto \Sigma_1^{1.9}$.
- Different regression methods give a slope in a range of $1.5 - 2.3$.

What are (quenched) post-starbursts (QPSB) ?

- Weak O II, Hα emission: low ongoing star formation rates
- Strong Balmer absorption (Hδ, Hγ,Hβ): high recent star formation
- Are ideal for testing merger-driven AGN feedback

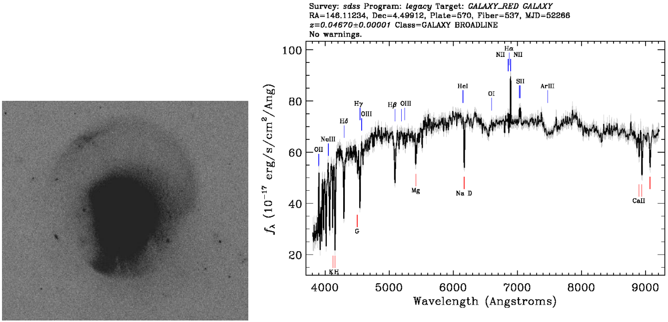

Figure: **Left:** HST WFC3 image **Right:** SDSS spectra

Sample properties of post-starburst galaxies

PSB galaxies as a class differ strongly from normal SDSS galaxies and further that the various types of PSB of galaxies differ from one another depending on how the samples are selected.

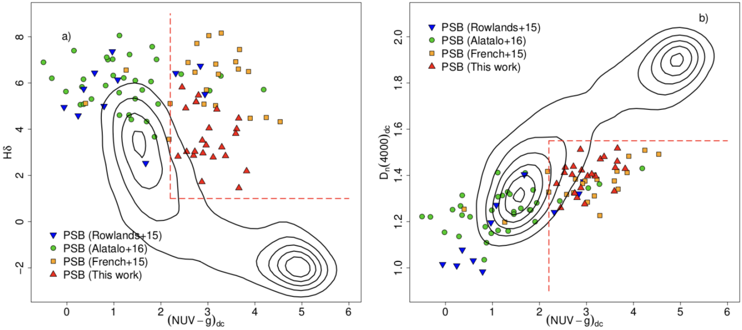

Sample properties of post-starburst galaxies

PSB galaxies as a class differ strongly from normal SDSS galaxies and further that the various types of PSB of galaxies differ from one another depending on how the samples are selected.

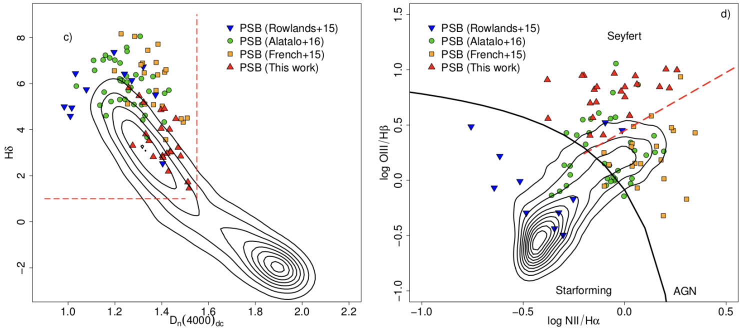

The distribution of gas fractions of Seyfert PSBs is significantly different from that of non-PSBs

- Seyferts (AGNs) have broad distribution of gas fraction.
- A higher proportion of Seyfert PSBs have gas fraction fractions below $\sim 10\%$.

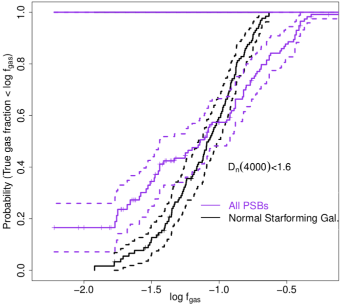

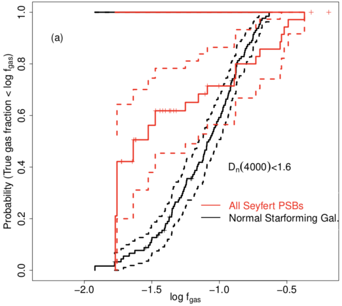

If there is an AGN effect on gas, it must at lower SSFR (i.e., delayed AGN feedback).

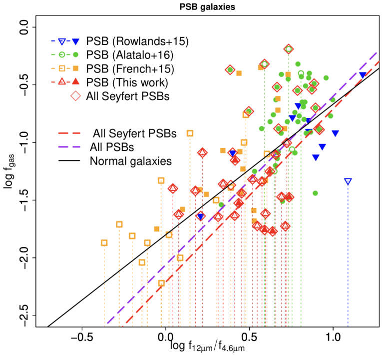

- Stellar populations younger than 0.6 Gyr dominate the 12 emission.
- Same correlation is at work: lower molecular gas fractions means lower sSFR or dust-heating.
- The gas fraction trend for AGN is similar to that of star forming galaxies.

Very preliminary: the AGN accretion rate is correlated with the molecular gas fraction.

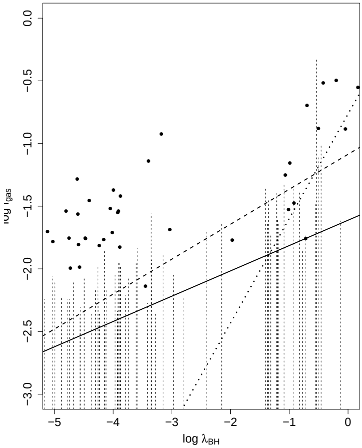

- Better data are needed.

Summary

- Used Random Forest to classify galaxies into real bulges and pseudobulges using the bulge-types of 809 representative galaxies from the SDSS by Gadotti (2009).
- Used structural and stellar population predictors that can easily be measured without image decomposition
- Classified $\sim 45,000$ face-on SDSS galaxies above 10^{10} $M_{\odot}$ and at $z < 0.07$ into real or pseudobulges with $93 \pm 2\%$ accuracy.
- Showed that the pseudobulge fraction decreases with AGN line ratio signatures indicating pure star formation ($\approx 55\%$) to AGN-dominated ($\approx 5\%$). $\sim 75 - 90\%$ of AGNs identified by BPT are hosted by galaxies with real bulges.
- The AGN fraction and the accretion rates onto them are linked to both on star formation and bulge types.

Bulge types of the COLD GASS sample

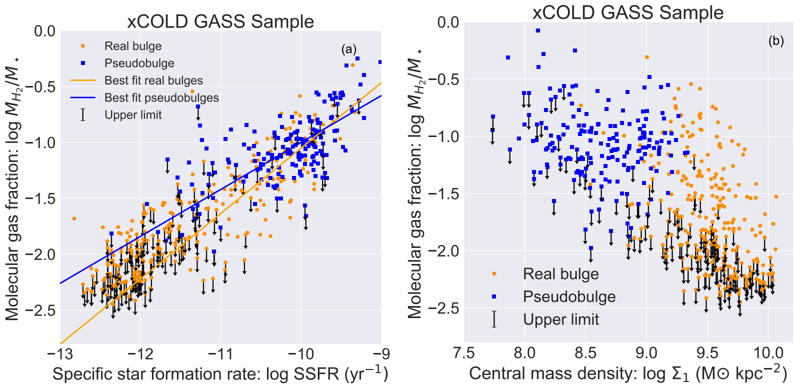

The HI gas fractions in AGNs are the same as that of star forming galaxies.

- Ellison+18 studied HI stacks of 1562 AGN from the Arecibo Legacy Fast ALFA (ALFALFA) survey.

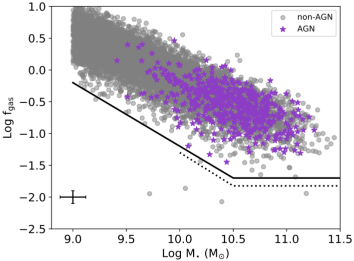

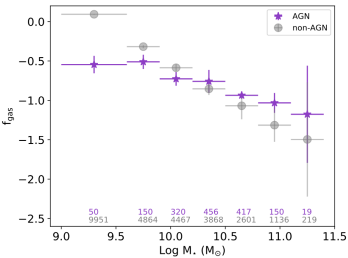

Ellison+18 did not find a correlation between AGN accretion and HI gas fraction.

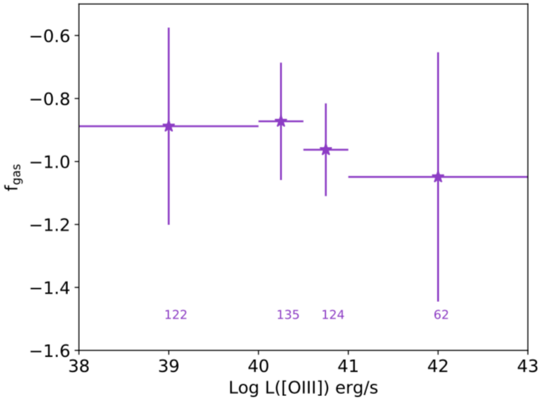

PG quasars have the same gas fraction as starforming galaxies.

- Shangguan, Ho, & Xie 2018 (at PKU) using dust mass found that most (90%) quasar hosts have gas fractions similar to those of massive, star-forming galaxies (See also Xia+12).

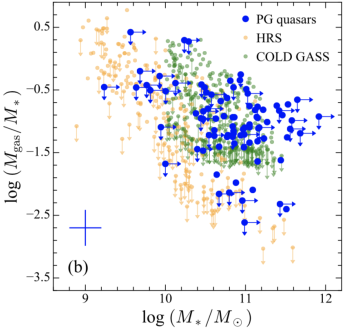

Shangguan+18 did not find a correlation between AGN accretion and gas fraction.